*34th EPS Conference on Plasma Phys. Warsaw, 2 - 6 July 2007 ECA Vol.**31F**, P-4.153 (2007)*

Experimental Conditions of ECRH and Magnetic Configuration for Efficient Electron Heating in Large Helical Device

T. Shimozuma[1], S. Kubo[1], S. Inagaki[2], Y. Yoshimura[1], H. Igami[1], T. Notake[3], I. Yamada[1], K. Narihara[1], K. Ida[1], S. Muto[1], N. Tamura[1], M. Yokoyama[1], T. Mutoh[1], A. Komori[1], and LHD Experimental Group

[1]*National Institute for Fusion Science, 322-6 Oroshi-cho, Toki-City, Gifu 509-5292, Japan*

[2]*Kyushu University, Research Institute for Applied Mechanics, 6-1 Kasuga-kouen, Kasuga-City, Fukuoka 816-8580, Japan*

[3]*University of Fukui, Research Center for Development of Far-Infrared Region, Bunkyo 3-9-1, Fukui 910-8507, Japan*

Achievement of high electron temperature and control of electron temperature gradient by ECRH is particularly important in view of not only obtaining high performance plasmas, but also studying fusion relevant low collisionality plasmas. In Large Helical Device (LHD), a magnetic configuration with inward-shifted magnetic axis had to be used for central heating by ECRH due to the maximum magnetic field limitation [1]. In the latest experimental campaign, sub-cooling of the helical coils expanded a possible operational regime of magnetic configuration.

In this paper, the relation between attained electron temperature and the magnetic configuration is studied experimentally and analytically in order to achieve higher core electron temperature by ECRH. Over 10keV core electron temperature has been obtained in the more preferable magnetic configuration expected by ray-tracing calculations.

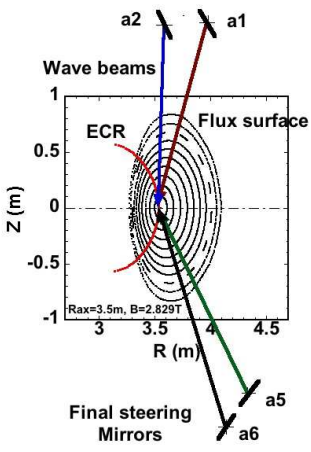

Fig. 1: Magnetic flux surface, ECR and ray beams from final steering mirrors are illustrated.

The ECRH system of LHD consisted of nine gyrotrons (two 82.7 GHz / 0.45 MW / 2 s, three 84 GHz / 0.8 MW / 3 s, one 84 GHz / 0.2 MW / 1000 s and three 168 GHz / 0.5 MW / 1 s), transmission lines and quasi-optical antennas. Total injection power exceeds 2 MW. There are two kinds of the transmission line used in LHD ECRH system. One is composed of a corrugated waveguide with 88.9 mm in diameter and some quasi-optical components. These transmission lines are connected to upper-port antennas (a1 and a2 antennas in Fig. 1). Another consists of an evacuated corrugated waveguide with 31.75 mm in diameter. The narrower lines transmit

millimeter-wave powers from the 84 GHz / 0.8 MW gyrotrons to the lower-port antennas (a5 and a6 antennas in Fig. 1). Because of a restriction of the injection configuration, the EC-beams from upper-port and lower-port antennas have to be injected with grazing incidence angle on the ECR. Accordingly, a little difference of the injection angle or location of focal point possibly leads to big variation of ECRH power deposition profile. Optimization of the ECR layer, magnetic configuration and antenna focal position is required, when high electron temperature at the plasma center is intended by strongly focused EC beams, in special.

When the electron temperature surpasses 10 keV, the absorption location of ECRH power moves to the higher magnetic field region because of the relativistic down-shift of ECR. The magnetic field strength for ECR increases with an increase of relativistic factor γ of resonant electrons. Figure 2 shows the relation between a non-relativistic ECR and the magnetic axis in two typical magnetic configurations of LHD. In case a), which corresponds to the case with a toroidally averaged magnetic axis: $R_{ax} = 3.5$ m and a magnetic field strength: $B_0 = 2.829$ T , The magnetic axis locates on the low field side of non-relativistic ECR. In case b)($R_{ax} = 3.5$ m, $B_0 = 2.931$ T), in contrast, the magnetic axis is set on its high-field side. When the central electron

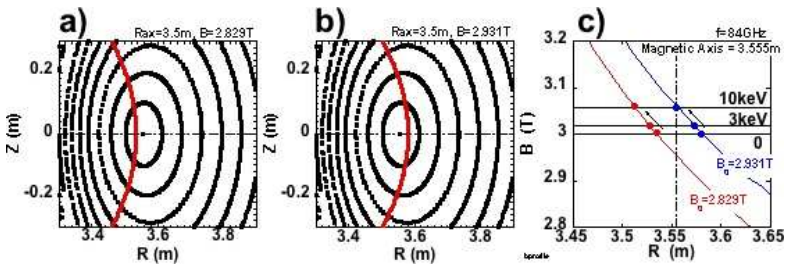

Fig. 2: Relation between non-relativistic ECR (red curves) and magnetic axis in $R_{ax} = 3.5$ m, a) $B_0 = 2.829$ T and b) $B_0 = 2.931$ T. Profiles of the field strength are plotted as a function of the major radius,R, in c).

temperature increases by ECRH, power absorption region will shift to higher-field side. The profiles of the magnetic field strength are plotted as a function of the major radius, R, in Fig. 2 c). The resonance magnetic field are also indicated by closed circles for the energy of 3 keV and 10 keV. It is clearly shown that on-axis heating will be kept in case b) even if the temperature increases, but that off-axis heating will occur with the temperature increase in case a).

Ray-tracing calculation clarifies the change of the absorption region by magnetic configuration more realistically. In the calculations, real 3-dimensional LHD magnetic field was used. For ray calculation the dispersion relation of cold plasma was used. While, the weakly relativistic dispersion relation for quasi-perpendicular injection was used for the calculation of the absorption. Profiles for the calculations were assumed to be a rather peaked temperature profile such as $T_e(\rho) = T_{e0}(1-\rho^2)^2$ and a flattened density profile such as $n_e(\rho) = n_{e0}(1-\rho^8)^2$, where ρ is the normalized minor radius. The focal position of the EC beam was specified by R_{foc}, which means

focal point on the equatorial plane. Figure 3 is an example of calculated absorption mappings on the ρ-R_{foc} plane for the antenna a1 in Fig.1. In the case of 2.83 T (a), the minimum ρ of a strong absorption region moves outward with the temperature increase. In the case of 2.93 T, the deposition region expands near the center depending on the temperature rise with the same antenna setting. The configuration b) has an advantage over a) for the efficient central heating on higher temperature. This tendency is also noticed in the calculation by using all the other antennas.

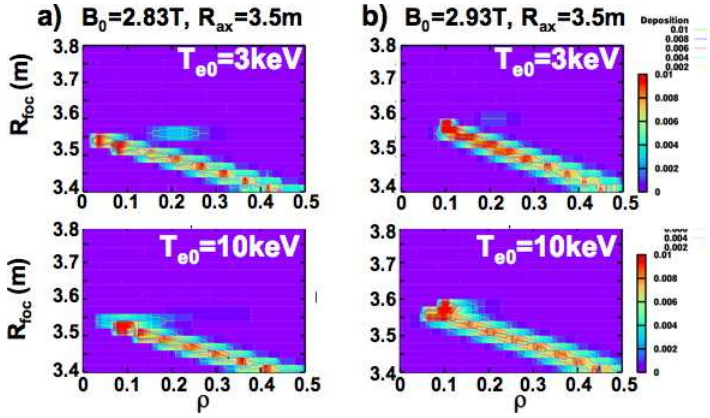

Fig. 3: EC wave absorption is mapped on ρ and R_{foc} plane for two magnetic configurations of (B_0, R_{ax}) =(2.83 T, 3.5 m) and (2.93 T, 3.5 m) . Calculations for two central temperature, 3 keV and 10 keV are plotted for each configuration. Red parts correspond to higher absorption region.

In the recent experiments in LHD, sub-cooling of the helical coils allowed higher magnetic field on the axis, leading to expansion of the freedom of the magnetic configuration. Plasma production and heating via fundamental and second harmonic ECR was performed by centrally focused ECRH (Power was about 1.6 MW) in the new configuration of R_{ax}=3.5 m, B_0=2.931 T, which was expected to be preferable to achieve high core temperature. In Fig. 4, profiles of the electron temperature and density are shown. The temperature profile was obtained by Thomson scattering and the density profile was measured by the FIR laser interferometer. The electron temperature profile is a centrally peaked profile with a central value of about 9 keV, while the density profile shows rather flat or hollow one around the center.

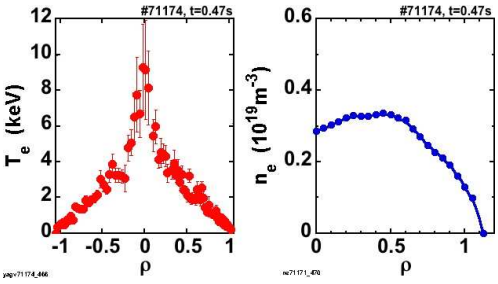

Fig. 4: Electron temperature and density profiles of high T_e shot.

Figure 5 shows the dependence of the central electron temperature T_{e0} on square root of ECRH power normalized by line-averaged density, $\alpha \equiv (P_{ECH}/\bar{n}_{19})^{\frac{1}{2}}$, for plasmas produced and sustained by only ECRH power in past experimental shots, where P_{ECH} is ECRH power in MW and $\bar{n}_{19}$ is line-averaged electron density in 10^{19} m^{-3}. The difference of the symbols corresponds to the magnetic configurations: 1) (R_{ax}, B_0)=(3.5 m, 2.829 T), small close circles, 2) (3.5 m, 2.931 T), triangles, 3) (3.53 m, 2.907T), large closed circles, 4) (3.53 m, 2.951 T), inverted triangles. The data points are divided into two groups, one shows almost linear de-

pendence on α and another shows improvement to high temperature state. For R_{ax}=3.53 m, the higher is the magnetic field, the smaller α is so that the improvement may occur.

In R_{ax}=3.5 m cases, such improvement occurs in higher α value than in 3.53 m case, and it was not observed in lower magnetic field of B_0=2.829 T. The configurations 2) and 4) are the case in which the magnetic axis located on the high field side of ECR, and 1) is the case in which the axis locates on the low field side. The configuration 3) corresponds to on-axis ECR. A threshold of transition from low to high temperature looks to depend on the magnetic configurations.

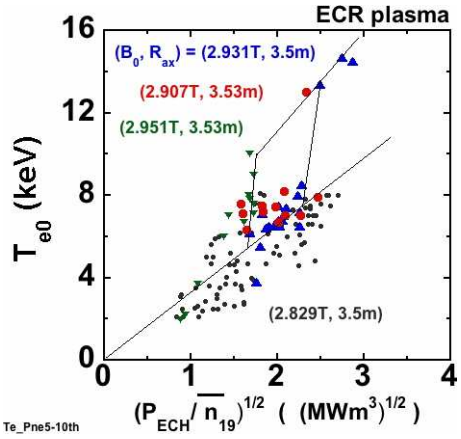

Fig. 5: Attained T_{e0} is plotted as a function of square root of ECRH power divided average density for different magnetic configurations.

Related with the existence of natural islands in core plasma, an interesting phenomenon was observed. In the magnetic configuration 3), reducing of the 2/1 island size by the external coil field realizes high central T_e, as shown in Fig. 6 a) and b). These data are clearly divided into two groups, and improvement of core temperature and even transition to high-T_e occur only with a reduced island.

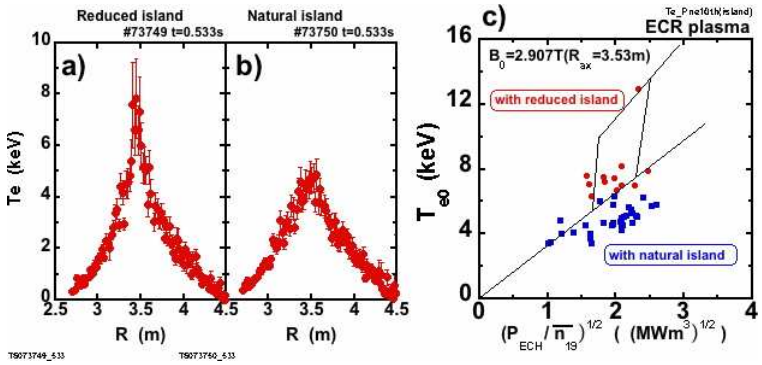

Fig. 6: Electron temperature profiles with a) reduced island and b) natural island. Attained T_{e0} is plotted for with and w/o island.

In summary, sub-cooling of the helical coils extends operation regime of magnetic configuration, which allows a preferable configuration taken account of the relativistic down-shift of ECR in over 10 keV electron temperature. Achieved electron temperature in the center shows two dependences on the density normalized ECRH power. The transition between two state is affected by the magnetic configurations. Attained peak temperature is partly affected by with or without a natural island.

This work was mainly performed under the budget codes NIFS06ULRR501-3 and partially supported by a grant-in-aid for scientific research of MEXT JAPAN, 2007 .19560051.

References

[1] T. Shimozuma, S. Kubo, H. Idei, S. Inagaki *et al.*, Nucl. Fusion **45**, 1396 (2005).